Effective doping of single-layer graphene from underlying SiO_2 substrates

Yumeng Shi,[1] Xiaochen Dong,[1,2] Peng Chen,[2] Junling Wang,[1] and Lain-Jong Li[1,*]
[1]*School of Materials Science and Engineering, Nanyang Technological University, Singapore, 639798*
[2]*School of Chemical and Biomedical Engineering, Nanyang Technological University, Singapore, 637459*
(Received 22 January 2009; published 3 March 2009)

When a single-layer graphene (SLG) is on SiO_2 substrates, the charge exchange at their interface results in a dipole, which direction strongly depends on the contact potential difference between the SLG and the substrates. Due to the longer experimental charge screening length of SLG than its thickness, the charge redistribution imposes effective *p* or *n* doping to SLG films. The substrate-dependent doping of SLG films is further confirmed by Raman and electrical measurements. Also, the unique electronic structures of SLG films make them sensitive to the doping rather than effective gating from the SiO_2 substrates.

DOI: 10.1103/PhysRevB.79.115402 PACS number(s): 79.60.Fr, 78.67.Ch

Graphene-derived nanomaterials are promising for applications such as atomically thin transistors, sensors, and other nanoelectronic devices. Since the discovery of single-layer graphene (SLG),[1] it has attracted intensive interest due to its two dimensionality and unique physics including quantum spin Hall effect,[2] phase-coherent transport,[3] bipolar supercurrent,[4] suppression of the weak localization,[5] and deviation from the adiabatic Born-Oppenheimer approximation.[6] The unique structure and properties of graphene offer unprecedented opportunities and potentials in fundamental studies as well as in future nanoelectronics.

Both theoretical and experimental results have demonstrated that the Fermi energy shift of SLG can be achieved by deliberate doing from metal,[7] gas molecules,[8] or electrical gating.[9,10] The possibility to open the energy gap in SLG through the perturbations from underlying substrates[11] has attracted lots of discussions.[12] Moreover, the effect of SiO_2 substrate has been ignored for a long time until a recent discovery that the surface SiO^- bonds efficiently gated the organic thin-film transistors.[13] For the SLG films deposited on SiO_2 substrates, perhaps unexpected from its perfect two-dimensional structure, the carrier density inhomogeneity has been identified and attributed to either the intrinsic mechanical ripples in the SLG sheet[14] or the charged impurities in the insulating dielectrics.[15–18] Although the screening of the substrate charge impurity by graphene layers has been investigated by theoretical[19–21] and experimental[22,23] works, the impacts of the underlying SiO_2 substrate to graphene films are not fully elucidated. Herein, we scrutinized this issue using electrostatic force microscopy (EFM), Raman spectroscopy, and electrical characterizations. Our results suggest that the effective doping from the underlying substrate is predominant rather than the effective gating[13] from substrates. It is concluded that the contact potential difference between SiO_2 substrates and SLG films controls the direction of the dipole formed at the interface. The substrate-induced electron injection (depletion) in SLG films actually imposes effective *n*-(*p*-) doping to the SLG films.

SLG films were obtained using the micromechanical exfoliation technique.[1] In brief, natural graphite flakes (from NGS) were repeatedly cleaved with adhesive tapes and then transferred to various SiO_2 substrates. We verified the SLG films using Raman spectroscopy and atomic force microscopy (AFM), as previously described.[24,25] Raman measurements were performed at room temperature in a WITEC confocal spectrometer with a 488 nm excitation laser operated at a low power level (~1 mW) in order to avoid any heating effect. The EFM study was performed by a dual-pass technique in tapping mode. Topography information was acquired in the first scan; the second scan was then performed while the tip was maintained at a constant distance ~30 nm above the surface based on the recorded profile. During the second scan (interleave scan), a dc voltage is applied to the tip. The long-range electrostatic force between the tip and the sample surface alters the tip resonance frequency, inducing a change in both phase and amplitude signals. Recording the phase shift reveals information about charge/potential distribution on the sample surface. An Asylum Research model MFP-3D system with Olympus (OMCL-AC240TM) Pt-coated cantilevers is used for this experiment. The tip curvature radius is ~15 nm, the quality factor is ~190, and the resonance frequency is ~70 kHz. EFM can map out the phase shift ($\Delta\phi$) of the cantilever, a lag between the drive frequency, and the cantilever oscillation. The $\Delta\phi$ is related to electrical force gradient (dF/dz) by the equation[26] $\tan(\Delta\phi) \sim (k/Q)(dF/dz)$, where Q and k represent the quality factor and the elastic constant of the cantilever and z is the distance between the tip and the sample surface. Figure 1(a) schematically shows the tip-sample system in our EFM setup. When the capacitive force dominates, the electrostatic force F can be normally described as[26]

$$F \approx \frac{1}{2}\frac{\partial C}{\partial z}\Delta V^2, \tag{1}$$

where C is the capacitance of the tip-sample system and ΔV is the potential difference between the tip and the sample ($\Delta V = V_{tip} - V_0$). V_{tip} is the voltage applied to the tip and V_0 is actually the contact potential difference between the sample and the tip. ($V_0 = \Phi_{sample} - \Phi_{tip}$, where Φ represents the Fermi level of the materials.)

The phase shift can then be derived as[27]

$$\Delta\phi = -\arcsin\left[\frac{Q}{2k}\frac{d^2C}{dz^2}(\Delta V)^2\right]. \tag{2}$$

As seen from Eq. (2), the minimum phase shift occurs when $V_{tip} = V_0$. Therefore, V_0 is obtained by fitting the phase-

 ©2009 The American Physical Society

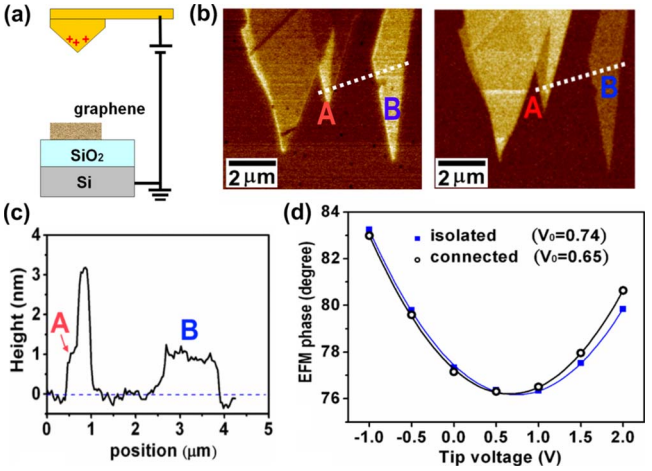

FIG. 1. (Color online) (a) Schematic illustration of EFM experiments. (b) The typical EFM images (left: V_{tip} is −1.5 V and right: V_{tip} is +1.5 V) for the graphene films on a SiO_2 substrate, where A and B represents the SLG connected to FLG films and the isolated SLG. (c) AFM cross section showing that the SLG films A and B are with the same thickness ~0.9 nm. (d) EFM phases as a function of V_{tip} for the SLG samples A and B. The V_0 was obtained by fitting to data points using the equation $\Delta\phi = -\arcsin[S(V_{tip}-V_0)^2] + T$.

shift data at different V_{tip} to the following equation:[27]

$$\Delta\phi = -\arcsin[S(V_{tip} - V_0)^2] + T, \tag{3}$$

where S is related to the parameter $(Q/2k)(d^2C/dz^2)$ and T is the offset in experimental measurements. The value of V_0 can be determined from the valley point of the fitted curve. The SiO_2 substrates [300 nm thermal oxide on As-doped Si (0.001–0.005 Ω cm)] with various values of V_0 (0.86, 0.50, 0.19, and 0.10 V) were selected. It is noted that the values vary with the method of growing SiO_2 and the cleaning process of SiO_2 surface. It is believed that the impurities or surface chemical bonds may cause the difference in V_0. We have also intentionally modified the surface of SiO_2 substrates with *m*-aminophenyl trimethoxysilane, where the V_0 for the modified substrates can be extended to −0.12 V.

SLG films obtained from mechanical exfoliation sometimes are in junction with the few-layer-graphene (FLG) films. We first show that the V_0 of the isolated SLG is different from that of the SLG connected to FLG films. Figure 1(b) demonstrates the typical EFM images (left: V_{tip} is −1.5 V and right: V_{tip} is +1.5 V) for the graphene films on a SiO_2 substrate, where A indicates a SLG connected to FLG films and B is an isolated SLG. The AFM cross-section profile [Fig. 1(c)] shows that the SLG films A and B are with the same thickness ~0.9 nm. It is worthy pointing out that this measured thickness falls into the range of reported SLG thickness which varies from 0.4 to 1.2 nm. The variation has been attributed to the AFM instrumental offset.[24] The isolated graphene B gives a brighter contrast than A at negative tip voltage, while a darker contrast is obtained if the tip voltage is positive. The nice fitting of the EFM results to Eq. (3) indicates that the capacitive force dominates under our EFM measurement conditions [Fig. 1(d)]. It allows us to

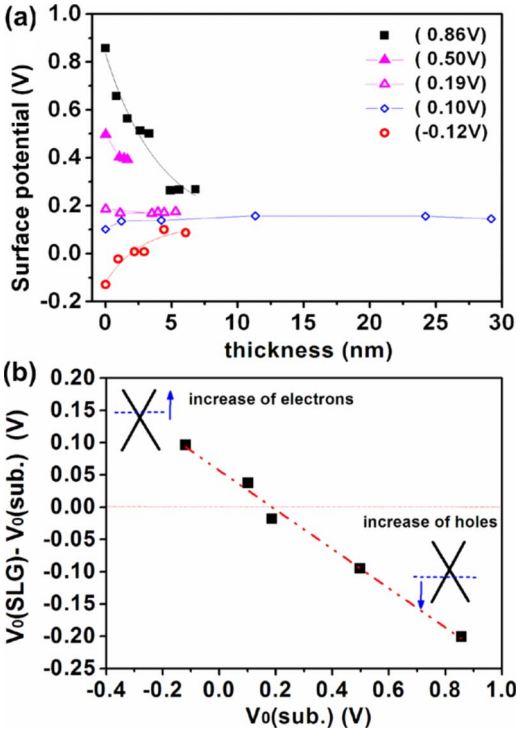

FIG. 2. (Color online) (a) The V_0 of few-layer graphene on SiO_2 substrates plotted as a function of their thickness, where we have examined six substrates with V_0=0.86, 0.50, 0.19, 0.10, and −0.12 V, respectively. (b) The change in the sample V_0 after SLG screening vs the initial V_0 of the substrates, where the positive value of $[V_0(\text{SLG}) - V_0(\text{sub})]$ indicates that the electron concentration in SLG is increased and the negative one indicates the decrease in electron concentration.

extract the V_0 for both samples. The V_0 of the isolated graphene B is ~0.74 V, which is higher than that of SLG A (0.65 V). Since both A and B are on the same substrates (with a V_0 of 0.89 V), the observed lower V_0 of SLG A must be attributed to the influence from the jointed FLG films which exchange carriers with the SLG A. Datta *et al.*[23] showed that the V_0 of FLG films increases with film thickness, approaching a bulk value for many-layer graphenes. Their results suggested that the SLG was not able to completely screen off the substrate V_0, likely owing to its intrinsically low carrier concentration. Similarly, our experiment demonstrates that the isolated SLG B can only partially screen off the substrate V_0 (0.89 V), giving a measured V_0 of 0.74 V. The better screening observed for SLG A (0.65 V) therefore suggests that the connected FLG films can provide carriers to the SLG for enhancing the screening effect.

It is likely that the screening effect is originated from the charge exchange (as a result of dipole formation[28]) between the graphene and the substrates. In principle, it is possible to control the polarity of the dipole—hence the type of the charge added into the graphene layers—by selecting the substrates with suitable V_0. To demonstrate the possibility, we examined the effect of various SiO_2 substrates on the V_0 of SLG and FLG. Figure 2(a) shows that the measured V_0 either increases or decreases with the sample thickness, depending on the initial V_0 of bare substrates (shown as the points at 0

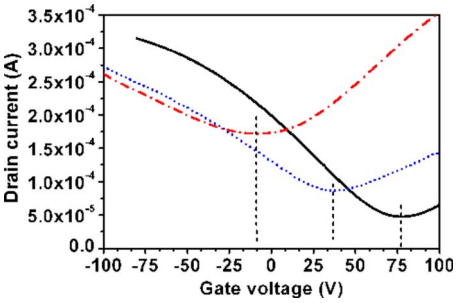

FIG. 3. (Color online) The transfer characteristics showing ambipolar conduction behaviors for the bottom-gated field-effect transistors based on the SLG films on SiO_2 substrates with (a) V_0 =0.86 V, (b) V_0=0.50 V, and (c) V_0=−0.12 V, respectively. The drain voltage was kept at 0.1V and the gate voltage was swept from 100 to −100 V. Thickness of SiO_2 was 300 nm, same as those used in EFM studies.

nm of thickness). In this experiment, we carefully selected the isolated SLG films or the ones connected to relatively small size of FLG films to reduce the unwanted doping effect from jointed FLG films. When the V_0 of bare SiO_2 substrate is above 0.19 V, the V_0 of FLG sheets on SiO_2 decreases with their thickness. Opposite trend was observed for the FLG sheets on the substrates with $V_0 < 0.19$ V. These results can be reasoned by the screening of various substrate potentials. Interestingly, when the substrate has a V_0 around 0.19 V, the measured V_0 of SLG or FLG films does not significantly vary with the sample thickness. We speculate that, in this case, the substrate exhibits a contact potential similar to the SLG or FLG films and therefore no significant charge exchange occurs between the graphene layers and the substrates. These results clearly suggest that the contact potential difference between the substrate and graphene layers drives the carrier redistribution at the substrate-graphene interface.

If a SLG or a thin FLG is used, the direct consequence of the incomplete potential screening (or charge exchange) is the electron injection or depletion in graphene. In a general sense, electron injection (depletion) is referred to the effective n-(p-) doping from substrates to FLG or SLG films. Figure 2(b) plots the change in the sample V_0 after SLG screening vs the initial substrate V_0, showing the substrate-dependent doping effect to SLG films. The positive value of $[V_0(\mathrm{SLG}) - V_0(\mathrm{sub})]$ indicates that the electron concentration in SLG is increased and the negative one represents the decrease in electron concentration. The effect of substrates demonstrated in Fig. 2(b) only refers to the change in carrier concentration (or shift of Fermi energy); for example, n doping occurs when $V_0(\mathrm{SLG}) - V_0(\mathrm{sub})$ is >0. The eventual doping state of the SLG, however, also depends on its initial carrier concentration (contributed from the possible p doping in ambient[1]). Nevertheless, the results postulate the possibility of tuning electronic property of graphene devices by substrates.

To examine the doping from substrates electrically, we prepared graphene field-effect transistors by evaporating source and drain electrodes (Au with a channel length ~15 μm) directly on top of the graphene films without using any photolithography process. The photoresist or other chemicals involved in photolithography or impurities resulting from these processes may give uncertain doping effects. Figure 3 shows the transfer characteristics (drain current vs gate voltage) for three transistor devices based on the selected SLG films on various substrates (with V_0=0.86, 0.50, and −0.12 V, respectively). The shape and the size of mechanically exfoliated graphene films are difficult to control. Consequently, the quantitative comparison between devices cannot be based on obtained absolute conductance. Fortunately, the gate voltage corresponding to the valley point in the transfer curves, which indicates the transition point between electron and hole conductions, allows us to characterize the relative Fermi level (or doping behaviors). The transfer curves clearly demonstrate that the ambipolar curve moves toward the negative gate voltage with the decreasing V_0 of substrates, suggesting the increase in electron concentration. This result is well corroborated with the conclusions drawn from Fig. 2(b). SLG on the substrate with a V_0 value of −0.12 V manifests n-doping characteristics as evidenced by the negative gate voltage at the valley point. This data postulate a simple strategy to make air-stable n-type graphene transistors via surface modification of substrates. It is worthy pointing out that we have also modified the SiO_2 surface (V_o=0.86 V) with phenyltriethoxysilane (PTS) which is normally used to block the free SiO^- group on SiO_2. The obtained V_o is around 0.89 V and the SLG devices exhibit highly p-doped characteristics. If the effective gating from SiO^- groups is pronounced, the SLG on PTS-modified substrates should exhibit less p-doped characteristics. Our

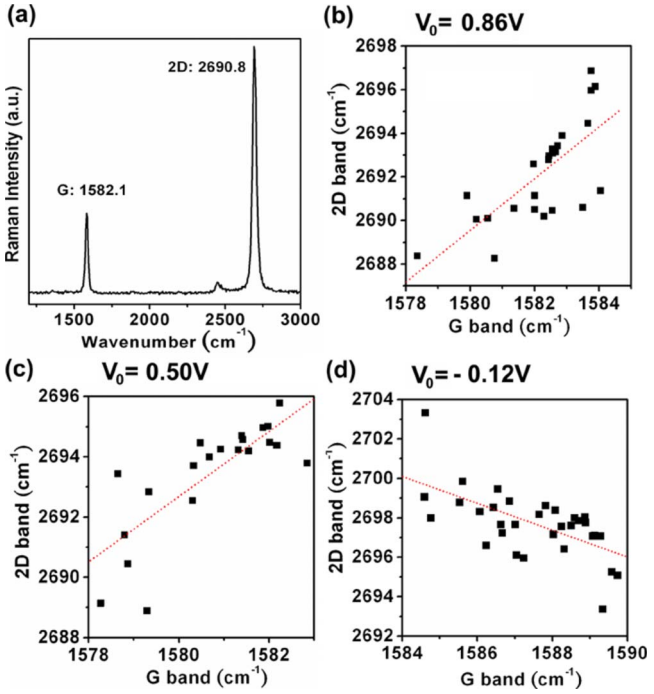

FIG. 4. (Color online) (a) Typical SLG Raman spectra obtained in ambient (excited with 488 nm laser). [(b)–(d)] Shown are maps of Raman 2D versus G frequencies for the SLG films on the SiO_2 substrates with (b) V_0=0.86 V, (c) V_0=0.50 V, and (d) V_0= −0.12 V, respectively. The upward (downward) trend represents that SLG is p doped (n doped).

results suggest that the effective gating[13] from the substrates is not as pronounced as the direct doping. This could be attributed to the unique semimetallic characteristics of SLG films which make them less sensitive to the effective gating from the SiO^- groups.

Raman spectroscopy is a powerful tool to reveal intrinsic optical properties and structures of various carbon materials. Figure 4(a) shows typical Raman spectra for a SLG obtained at room temperature with 488 nm laser excitation. The characteristic G ($\sim$1582 cm^{-1}) and 2D ($\sim$2690 cm^{-1}) Raman bands are sensitive to the presence of doping.[10,29] Electron and hole dopings not only impose shifts of the ambipolar curves for the SLG based devices but also have distinct effects on the Raman modes for SLG films. It has been reported that p doping caused upshifting for both G and 2D Raman frequencies, while n doping resulted in opposite shifting in G and 2D frequencies.[10,29] Based on these observations, the Raman 2D vs G frequency map has been used to distinguish the n or p doping to SLG films.[29] Figures 4(b)–4(d) map the 2D- and G-band frequencies measured at different locations of the SLG film on three substrates with V_0=0.86, 0.50, and −0.12 V, respectively. The data points in each graph can be fitted by a downward (or upward) line, showing that variation in 2D frequency inversely (or proportionally) correlates with variation in G frequency, where the downward (upward) line indicates that the SLG is n-(p-) doped. The Raman results for these SLG films are consistent with the electrical characterizations, confirming that n or p doping can be controlled by the substrates with various values of V_0.

In summary, we studied the V_0 of SLG on insulating substrates using EFM. It was found that graphene layers tend to screen off the potential of the underlying substrates as a result of the charge exchange (dipole formation) at their interface. The charge exchange leads to the doping in graphene films, which, in turn, modulates the electronic properties of the SLG films. The doping effect (p or n doping) is controlled by the contact potential difference between substrates and graphene. Such substrate-dependent doping was confirmed by electrical measurements for the graphene transistors made on various substrates.

We acknowledge with thanks the support from NTU, Singapore. We also acknowledge the support from A-Star SERC grant (Grant No. 072 101 0020) to P.C.

*ljli@ntu.edu.sg

[1] K. S. Novoselov, A. K. Geim, S. V. Morozov, D. Jiang, Y. Zhang, S. V. Dubonos, I. V. Grigorieva, and A. A. Firsov, Science **306**, 666 (2004).
[2] Y. B. Zhang, Y. W. Tan, H. L. Stomer, and P. Kim, Nature (London) **438**, 201 (2005).
[3] F. Miao, S. Wijeratne, Y. Zhang, U. C. Coskun, W. Bao, and C. N. Lau, Science **317**, 1530 (2007).
[4] H. B. Heersche, P. Jarillo-Herrero, J. B. Oostinga, L. M. K. Vandersypen, and A. F. Morpurgo, Nature (London) **446**, 56 (2007).
[5] S. V. Morozov, K. S. Novoselov, M. I. Katsnelson, F. Schedin, L. A. Ponomarenko, D. Jiang, and A. K. Geim, Phys. Rev. Lett. **97**, 016801 (2006).
[6] S. Pisana, M. Lazzeri, C. Casiraghi, K. S. Novoselov, A. K. Geim, A. C. Ferrari, and F. Mauri, Nature Mater. **6**, 198 (2007).
[7] G. Giovannetti, P. A. Khomyakov, G. Brocks, V. M. Karpan, J. van den Brink, and P. J. Kelly, Phys. Rev. Lett. **101**, 026803 (2008).
[8] F. Schedin, A. K. Geim, S. V. Morozov, E. W. Hill, P. Blake, M. I. Katsnelson, and K. S. Novoselov, Nature Mater. **6**, 652 (2007).
[9] J. Yan, Y. Zhang, P. Kim, and A. Pinczuk, Phys. Rev. Lett. **98**, 166802 (2007).
[10] A. Das, S. Pisana, B. Chakraborty, S. Piscanec, S. K. Saha, U. V. Waghmare, K. S. Novoselov, H. R. Krishnamurthy, A. K. Geim, A. C. Ferrari, and A. K. Sood, Nat. Nanotechnol. **3**, 210 (2008).
[11] S. Y. Zhou *et al.*, Nature Mater. **6**, 770 (2007).
[12] E. Rotenberg, A. Bostwick, T. Ohta, J. L. McChesney, T. Seyller, and K. Horn, Nature Mater. **7**, 258 (2008).
[13] L. L. Chua *et al.*, Nature (London) **434**, 194 (2005).
[14] M. I. Katsnelson and A. K. Geim, Philos. Trans. R. Soc. London, Ser. A **366**, 195 (2008).
[15] E. H. Hwang, S. Adam, and S. Das Sarma, Phys. Rev. Lett. **98**, 186806 (2007).
[16] K. Nomura and A. H. MacDonald, Phys. Rev. Lett. **98**, 076602 (2007).
[17] S. Adam, E. H. Hwang, V. M. Galitski, and S. D. Sarma, Proc. Natl. Acad. Sci. U.S.A. **104**, 18392 (2007).
[18] T. Ando, J. Phys. Soc. Jpn. **75**, 074716 (2006).
[19] I. S. Terekhov, A. I. Milstein, V. N. Kotov, and O. P. Sushkov, Phys. Rev. Lett. **100**, 076803 (2008).
[20] M. M. Fogler, D. S. Novikov, and B. I. Shklovskii, Phys. Rev. B **76**, 233402 (2007).
[21] M. I. Katsnelson, Phys. Rev. B **74**, 201401(R) (2006).
[22] T. Ohta, A. Bostwick, J. L. McChesney, T. Seyller, K. Horn, and E. Rotenberg, Phys. Rev. Lett. **98**, 206802 (2007).
[23] Sujit S. Datta, Douglas R. Strachan, E. J. Mele, and A. T. Charlie Johnson, Nano Lett. **9**, 7 (2009).
[24] A. Gupta, G. Chen, P. Joshi, S. Tadigadapa, and P. C. Eklund, Nano Lett. **6**, 2667 (2006).
[25] A. C. Ferrari, J. C. Meyer, V. Scardaci, C. Casiraghi, M. Lazzeri, F. Mauri, S. Piscanec, D. Jiang, K. S. Novoselov, S. Roth, and A. K. Geim, Phys. Rev. Lett. **97**, 187401 (2006).
[26] J.-H. Kim, H. Noh, Z. G. Khim, K. S. Jeon, Y. J. Park, H. Yoo, E. Choi, and J. Om, Appl. Phys. Lett. **92**, 132901 (2008).
[27] C. H. Lei, A. Das, M. Elliott, and J. E. Macdonald, Nanotechnology **15**, 627 (2004).
[28] L. Chen, R. Ludeke, X. Cui, A. G. Schrott, C. R. Kagan, and L. E. Brus, J. Phys. Chem. **109**, 1834 (2005).
[29] C. Casiraghi, S. Pisana, K. S. Novoselov, A. K. Geim, and A. C. Ferrari, Appl. Phys. Lett. **91**, 233108 (2007).